



Microstructure and Wear Properties of Laser Treated Ni₃Al Coatings on Low Alloy Medium Carbon Steel

Naveed Akhtar¹ · Muhammad Afzal¹ · Rehan Akhter²

Accepted: 18 July 2018 / Published online: 3 August 2018
© Springer Science+Business Media, LLC, part of Springer Nature 2018

Abstract

Laser modification of nickel-aluminide (Ni₃Al) coatings on low alloy medium carbon steel substrate was carried out with the help of industrial CO₂ laser. The depth of the laser melted zone (modified surface) was controlled as a function of input energy by varying the laser beam travel speed. The laser treated specimens were characterized for microstructure, chemical composition, and micro-hardness profile with respect to the laser penetration depth. Microstructural examination revealed that the laser treated surface was composed of ultrafine grain structure which evolved as a result of laser re-melting and solidification (cooling) rate used in this experiment. Microhardness results showed that as the depth of the laser melted zone increases the hardness of the modified surface decreases and vice versa. Further, the wear behavior of the laser treated surface was also studied with the help of ball-on-disc tribometer and by selecting 2000 m sliding distance. Wear test showed that as the depth of laser melted zone increases the wear of the surface increases as well and vice versa. The possible reason behind this phenomenon was the migration of iron (Fe) atoms from substrate into the surface layer which resulted the dissolution of Ni₃Al coating particles in the surface layer and this was confirmed by the EDX analysis.

Keywords Laser modification · Re-melting · Microstructure · Microhardness · Wear · Nickel-aluminide

Introduction

Surface properties of metallic materials such as hardness, wear, friction, oxidation and corrosion resistance mainly depends on the chemical composition, and microstructure

✉ Naveed Akhtar
naveed3158@gmail.com

¹ NINVAAT, NCP Complex, Quaid-e-Azam University, Islamabad, Pakistan

² Pakistan Institute of Lasers and Optics, PO Box 505, Rawalpindi, Pakistan

of the surface. Many researchers [1–4] explored the possibilities of surface modification without making alteration in the bulk of materials. Historically, techniques like flame hardening, induction hardening, nitriding, carburizing, and carbonitriding etc. have been used for surface treatment of iron-base materials [5–8]. Although, these conventional techniques can enhance surface properties many times, however, at the same time these methods pose certain limitations. Therefore, an interest has been developed in advanced techniques such as laser treatment of the surfaces especially the coated surfaces [9–12].

Laser surface modification technique has already produced fascinating results as compared to the conventional methods [13, 14]. The parts fabricated through laser re-melting and deposition methods have shown superior strength, hardness, and tribological properties [15–18]. It became possible due to the modern lasers, which provide high energy density, small spot size with low and precisely controllable heat input that is used to produce thin hardened surface layer. In comparison with conventional surface hardening techniques, it offers low distortions, less residual stresses and surface oxidation during processing [19]. Hence, the laser modified components can be used for dies, moulds, structural parts, machine tools [20] and surgical equipments demanding superior resistance to wear, and hardness property at the same time [21].

Laser surface modification also offers many advantages over chemical vapor deposition (CVD) and physical vapor deposition (PVD) such as it does not require any vacuum, and parts of complex geometry and size can be treated with ease. Metallurgically it produces a fine microstructure having metastable phases with low level of porosity and inclusions [22]. Further, a narrow heat affected zone, and superior bonding (fusion) between the coating and the base metal are the added advantages [23, 24]. Many studies have shown better mechanical and tribological properties, which translate improved wear and friction behavior of the surface after laser modification [25–27]. There are many key parameters which affect the quality of the laser treated surface i.e. laser beam power, interaction time, relative travel speed etc. The depth of laser hardened surface can be controlled by the power and the dwell time of the laser beam.

In the present study ordinary low alloy medium carbon steel was locally modified to improve the hardness and resistance to wear and oxidation. Firstly, nickel-aluminide (Ni_3Al) coating was spread on the substrate specimens via thermal spraying technique. Subsequently, the coated surface was re-melted with the help of laser beam and solidified under different cooling rates. The laser treatment transformed the Ni_3Al coating layer into a freshly evolved composite layer having unique microstructure and improved wear properties.

Experimental Details

Substrate material

The substrate used for thermal spraying coatings and subsequent laser treatment has chemical composition close to AISI 4140 steel grade and the mean values are given in Table 1. This composition suggests that the base metal used for surface modification has low level of elemental and gaseous impurities [28]. Such quality was chosen purposefully, so that thermal spraying and subsequent laser re-melting may not generate undesirable side reaction products.

Table 1 Chemical composition of substrate used in this study

Element	C	Si	Mn	P	S	Cr	Mo	Ni	Cu	Al	Fe
Wt.%	0.39	0.26	0.88	0.01	0.03	1.4	0.23	0.40	0.12	0.03	~bal.

Coating Deposition by Thermal Spraying Process

The nickel-aluminide (Ni_3Al) coatings was deposited on the steel substrate by using Air Plasma Spraying system consisting of a 3 MB spraying gun. Initially, the specimens were grit blasted with alumina powder (particle size 30–40 mesh) to produce a rough surface on the substrate. Surface preparation before the thermal spraying is a pre-requisite step, which ensures good mechanical anchoring and adhesion bonding between the coating layer and the substrate. Subsequently, the specimens were preheated to ~ 150 °C just before the thermal spraying. Next, the substrate specimens were subjected to air plasma spraying (thermal spraying). The operating parameters used during thermal spraying process have been enlisted in Table 2. The nickel and aluminium powder was used in a ratio of 4:1 having apparent density 3.0 g/cm^3 . The particle size of the mixed Ni/Al powder was 50–100 μm . The coating was deposited at a standoff distance of 100 mm.

Laser Re-Melting Process

The nickel-aluminide (Ni_3Al) coatings deposited on substrate was re-melted by using a 2.5 kW transverse flow CO_2 laser. The key operating parameters used in this study for laser re-melting have been enlisted in Table 3. The power and spot size of the laser beam was kept constant in all the specimens. However, the beam travel speed and energy density was varied to get a different pool depth of the laser melted zone. During laser treatment the movement of the specimen was controlled through a CNC operated table. Argon was used as a shielding gas to protect the molten pool from oxidation and hydrogen pickup.

Table 2 Process parameters used for thermal spraying

Parameter	Value
Torch input power	60 kW
Current	600 A
Voltage	50 V
Plasma gas (Ar) flow rate	52.9 l/min
Secondary gas (H_2) flow rate	5.2 l/min
Powder feed rate	20 g/min
Carrier gas (Ar) flow rate	14.2 l/min
Torch to base distance	100 mm
Powder	Ni / Al

Table 3 Laser processing parameters used in this study

Sample ID	Power (W)	Travel Speed (mm/min)	Spot diameter (mm)	Beam coverage area (mm ²)	Focal length (mm)	Energy density (J/cm ²)	Power density (W/cm ²)
A	700	600	5	19.6	80	1.40×10^3	0.36×10^4
B		300				2.80×10^3	
C		150				5.60×10^3	

Characterization Tools

The localized chemical composition, phase analysis and microstructure of the coatings, and laser treated surfaces were studied with the help of optical microscope, field emission scanning electron microscope (SEM) equipped with energy dispersive X-ray (EDX) spectrometer, and X-ray diffractometer (XRD). The representative specimens of the laser treated surfaces were ground well on SiC papers, and polished with the help of 1.0 μm diamond paste. Finally, the samples were chemically etched in 2% Nital solution, and immediately examined.

Vickers microhardness of the laser treated specimens was measured by using metallographic samples. Hardness was measured both on the top surface and cross-sectional face normal to the laser track by selecting 500 g load. The HV value taken was an average of five measurements, and the distance between two consecutive indents was kept at 0.05 mm apart.

Wear Test

Unidirectional sliding wear test was performed on the laser treated surfaces. For this purpose a ball-on-disc type tribometer capable of data acquisition rate 1.00 Hz was used in this study. All the samples were weighed before and after the wear test. During the wear test a 100Cr ball of 6 mm diameter was slid in a circular path having 4 mm radius against the sample surface with a sliding speed of 20 cm/s. A normal load of 5 N was applied under the laboratory atmospheric conditions (temperature ~ 25 °C, humidity 50%). During the wear tests, the coefficient of friction force (μ) was continuously recorded, and plotted against time (s) and sliding distance (m). A total sliding distance of 2000 m was kept in all the samples. Wear properties such volumetric loss (V_{Wear}) and wear rate (K_v) was calculated with the help of eqs. 1 and 2, respectively.

$$V_{\text{Wear}} = \frac{W_1 - W_2}{d} \quad (1)$$

Where,

- W_1 weight of specimen before wear test, g
- W_2 weight of specimen after wear test, g
- d density, g/cm^3

$$K_v = \frac{V_{\text{Wear}}}{(\text{FN})S} \quad (2)$$

Where,

FN contact load in Newton, N

S sliding distance in meter, m

Surface profilometer was used to measure the depth and width of the wear tracks in order to calculate relative wear resistance. Similarly, wear tracks were also examined under the SEM to characterize the worn out surfaces.

Results and Discussion

Nickel-Aluminide Coatings Microstructure

The metallurgical examination of the as-sprayed nickel-aluminide coatings by using SEM showed some prominent features including the presence of irregular shaped porosity, un-melted Ni/Al particles, interfacial defects, and entrapped oxides of Ni and Al within the coating splats (Fig. 1). The EDX analysis of the coated specimen showed that coatings was composed of ~9.78% Al and ~90.22% Ni by weight. The thickness of the Ni₃Al coating layer was approximately 125 μm in all the specimens. Fig. 1c presents high magnification micrograph of the coating in cross-sectional specimen. It contained two distinct areas; light gray area is the Ni₃Al splats, whereas the dark area/black colour is the oxide of Ni and Al as confirmed by the EDX analysis (EDX Area-2). Moreover, some microcracks (poor adhesion) could also be seen at substrate-coating interface (Fig. 1b).

Laser Melted Zone Microstructure

The laser treated specimen showed three distinct regions under the scanning electron microscope as shown in Fig. 2. First, the laser melted zone (LMZ), second the heat affected zone (HAZ), and third was the base metal. There was a very narrow interface between the LMZ and HAZ named as fusion boundary. These regions can be distinguished with the help their unique microstructural features as well as on the base of microhardness values. The base metal showed almost equal amounts of ferrite platelets distributed inside the pearlite phase as shown in Fig. 2b. The laser melted zone showed newly developed ultrafine grain structure (Fig. 2c). The process parameters used during the laser re-melting and cooling rate was primarily held responsible for the microstructural features evolved inside the melted zone.

The microscopic observations made on laser treated surface revealed a good homogeneous surface without any micro-crack, porosity or other discontinuities. Moreover, a continuous and defect free interface was observed between the substrate and the laser melted layer (Fig. 2d). The coating-substrate interface gets improved due the migration/diffusion of Fe atoms into the coating layer. Hence, it can be concluded that laser

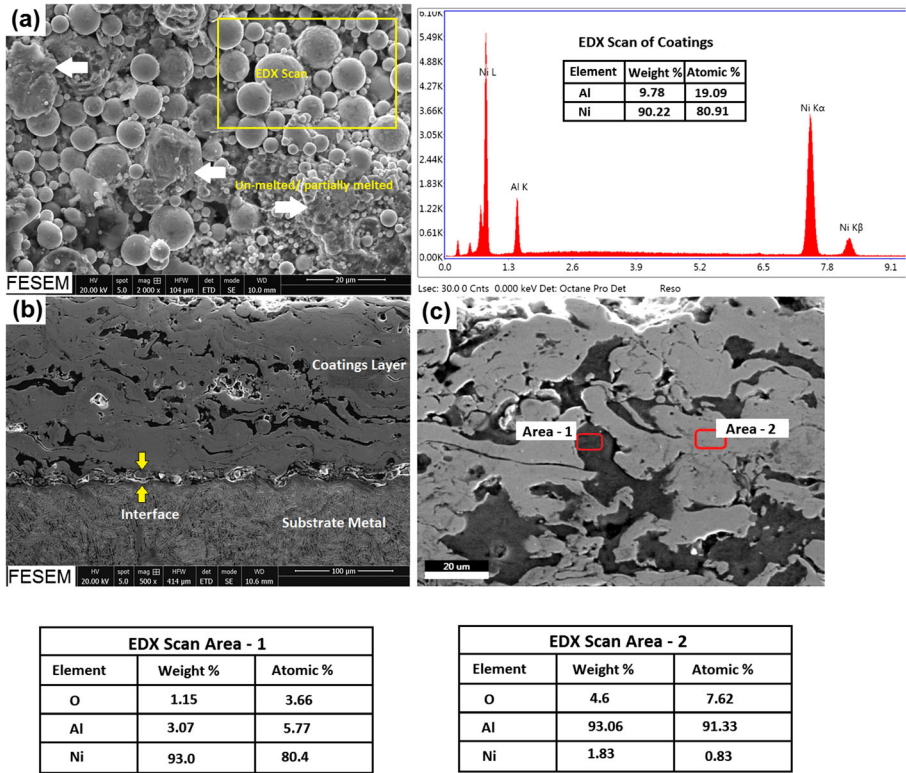


Fig. 1 SEM micrographs of thermal spraying Ni₃Al coatings, **a** high magnification image of Ni₃Al coatings and EDX scan, **b** cross-sectional view of the etched specimen at 500X, **c** coating splats and entrapped oxides along with EDX analysis of Area-1 & Area-2

treatment improved the properties of the Ni₃Al coatings deposited by plasma (thermal) spraying.

It was observed that laser beam travel speed used during the melting influenced the bead depth. In specimen-A bead depth was 569.6 μm, which was processed at 600 mm/min. The relative beam travel speed was kept at 300 mm/min and 150 mm/min in specimen-B and specimen-C, respectively. The bead depth recorded was 704.2 μm, and 1059 μm in specimen-B and specimen-C, respectively. As given in Table 3, the energy density in respective specimen-A, specimen-B and specimen-C was 1.4 × 10³, 2.8 × 10³, and 5.6 × 10³ J/cm². It means, input energy is directly related to relative travel speed of the laser beam. As the travel speed of the laser beam decreases, the input energy increases, correspondingly.

The microhardness profile taken in a cross-sectional specimen of each laser treated surface has been given in Fig. 3. The maximum microhardness values of specimen-A, specimen-B and specimen-C was 602 HV, 556 HV, and 367 HV, respectively. The hardness was increased 84%–201% in laser treated specimens with respect to the base metal. The graphical representation of microhardness as

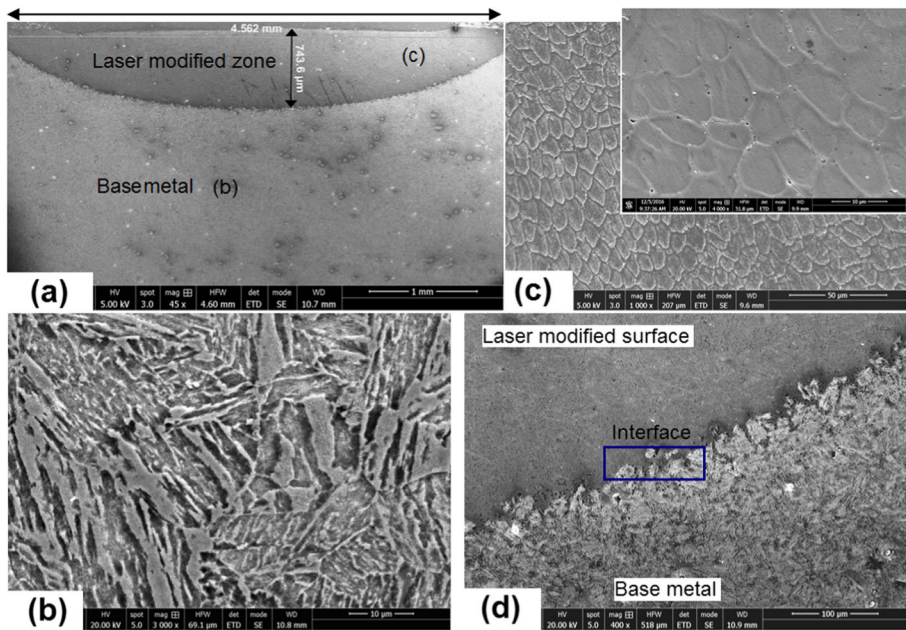


Fig. 2 **a** Laser treated specimen showing the depth of melted/modified zone, **b** base metal microstructure as viewed under the SEM, **c** Laser melted zone microstructure: inset showing high magnification image, **d** showing fusion boundary/interface between the base metal and laser melted zone

a function of laser melted zone depth (or laser travel speed) is shown in Fig. 4. The decrease in microhardness by increasing the depth of the laser melted zone can be correlated with the dilution of hard Ni_3Al coating particles inside the substrate matrix. It was also confirmed by the EDX analysis of all the three specimens and given in Table 4. From this table it is evident that the elemental concentration of Ni and Al is decreased in the order: specimen-A > specimen-B > specimen-C, whereas, Fe concentration was increased in the same order. Hence, it is concluded that by decreasing the laser beam travel speed the energy input increases as well, which in turn increases the melted zone depth, and consequently a decrease in micro-hardness was observed due to the dilution of Ni_3Al hard particles inside the surface layer.

The dilution of Ni_3Al particles with Fe atoms has also been confirmed by XRD pattern given in Fig. 5. The as-sprayed specimen showed prominent peaks of Ni_3Al (nickel aluminide) phase along with minor peaks of NiO (nickel oxide). The XRD pattern of laser treated specimen revealed that Ni_3Al particles in the surface layer have been decreased as shown by the peak intensities, and a large Fe (iron) peak was also observed in the laser treated specimen.

Wear Test Results

Friction coefficients of the three specimens were determined on the smooth polished surfaces by using ball-on-disc apparatus (as mentioned in subsection “[Results and Discussion](#)”). Friction coefficient (μ) is defined as the ratio between the measured

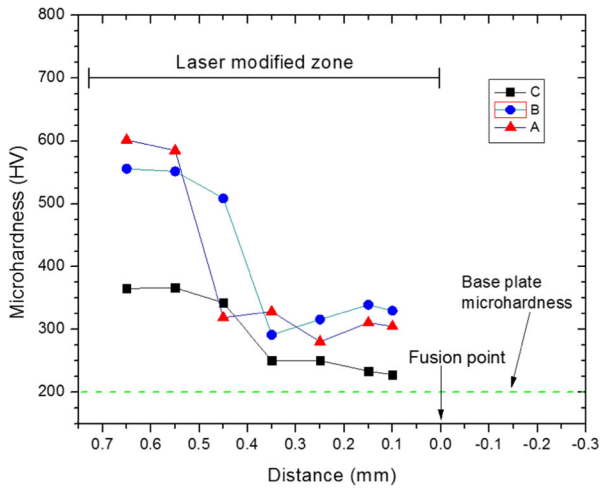


Fig. 3 Microhardness profile of laser treated specimens in cross-section

friction force during sliding (F), and the applied load (P). Figure 6 presents the variation of μ with respect to sliding distance at various beam travel speeds. These plots can also be used to predict the variations of wear loss against sliding distance or time. All of the three curves consist of two distinct stages, which are (1) running-in wear, and (2) steady-state wear. Initially, the friction coefficient increases with time to a maximum and then decreases to achieve a steady-state. However, the time taken to achieve the steady-state was different in three respective specimens.

The wear mass loss and the wear rate for all the samples were calculated by using the equations mentioned in subsection “Results and Discussion”.5. The results showed that the mass loss value and the wear rate of laser treated specimens depend on the degree of dilution of Ni₃Al coatings layer by the diffusion of Fe atoms from the substrate matrix. It is obvious from the fact that wear of coatings layer depends upon the laser beam penetration depth (or relative travel

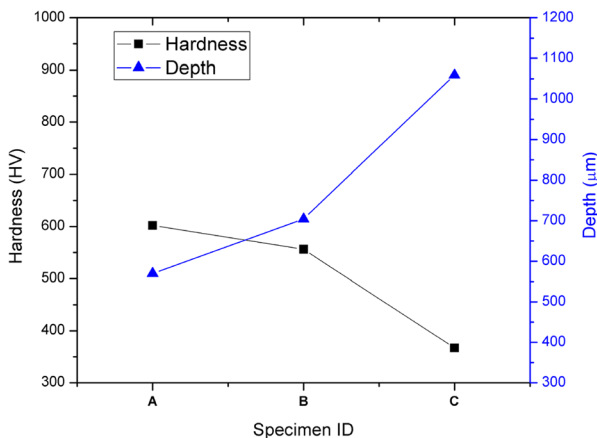


Fig. 4 Variation of micro-hardness with respect to depth of laser melted zone

Table 4 EDX analysis of the laser treated specimens near mid-thickness in cross-section

Element	Weight %		
	Specimen - A	Specimen - B	Specimen - C
Al	6.88	6.03	3.52
Cr	0.64	0.71	0.98
Fe	23.95	39.92	53.36
Cu	0.46	0.40	0.49
Ni	64.35	51.28	34.18
Mn	0.81	0.77	0.94

speed). Because laser beam travel speeds controls the input energy which correspondingly decide the penetration depth or dilution factor. A relationship between the wear rate and the laser beam travel speed or energy input has been plotted in Fig. 7.

It shows that the lowest mass loss was for the laser treated specimen-A, which has the least depth of the melted zone amongst the all samples. Lower the depth of the melted zone means abundance of Ni_3Al particles inside the modified surface layer. On the other hand, higher energy density will dilute the Ni_3Al coating layer by the diffusion of iron (Fe) atoms due to the melting of underneath steel substrate. Therefore, wear rate has also been increased by going from specimen-A towards specimen-C (Fig. 7).

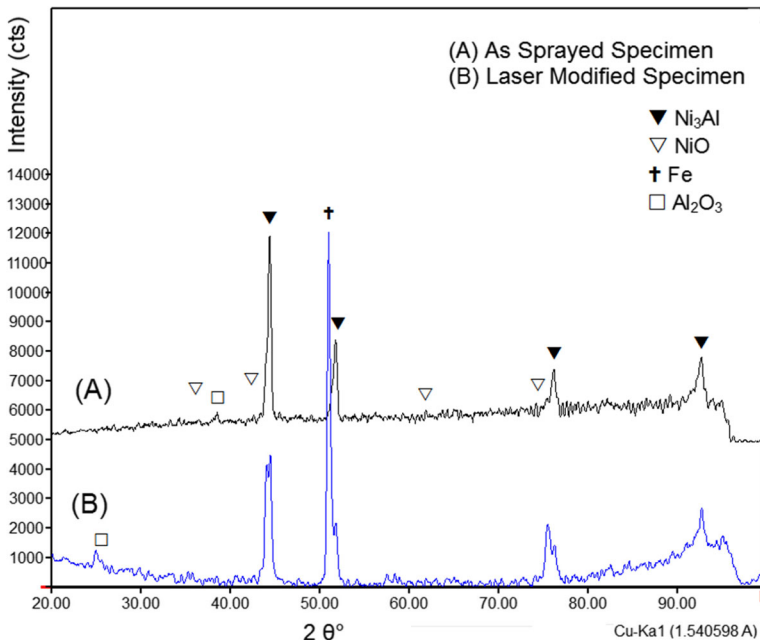
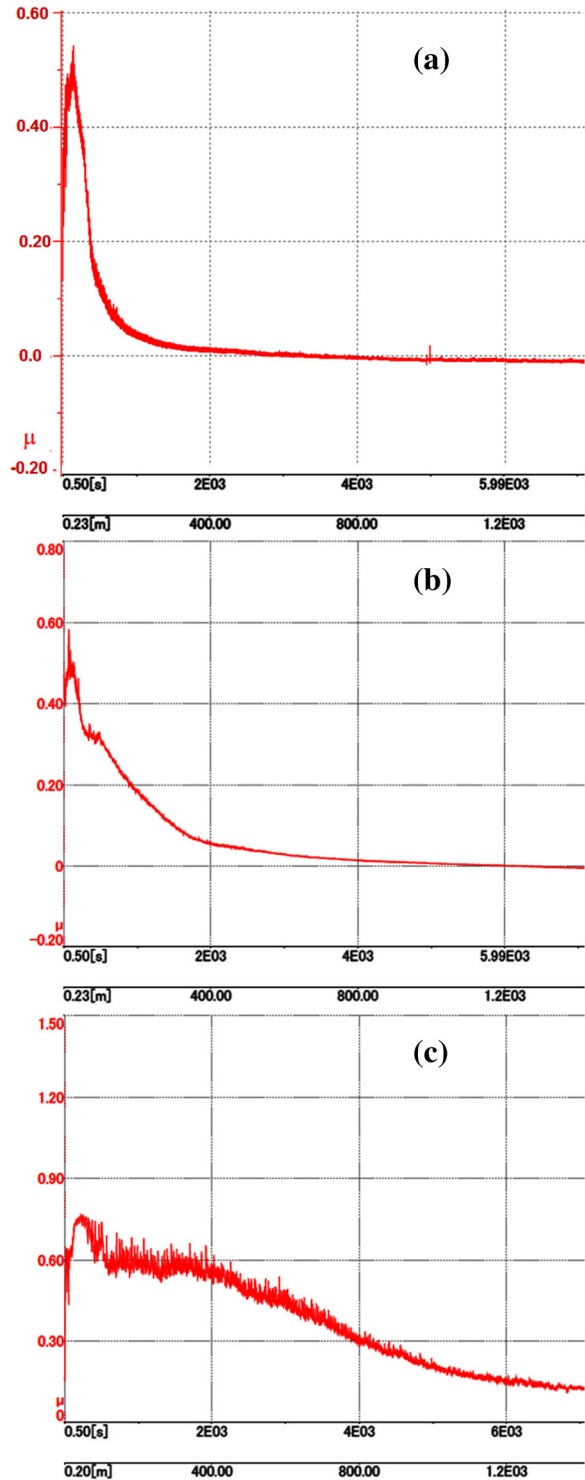
**Fig. 5** XRD patterns of as-sprayed specimen and laser treated (modified) specimen

Fig. 6 Friction coefficient versus sliding distance/time for laser treated specimens (polished surface)



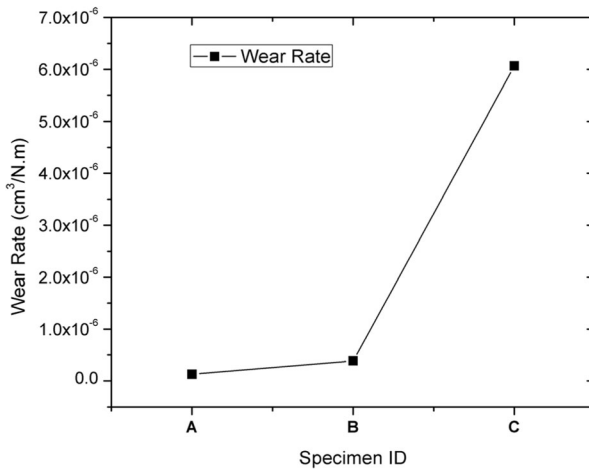


Fig. 7 Wear rate of laser treated specimens

Wear Fractography

Figure 7 presents the SEM fractographs of the worn surfaces after the 2000 m sliding wear test. Wear track width and the morphology of the worn surface of specimen-A is shown in Fig. 8a-b. Similarly, micrographs in Fig. 8c-d represent specimen-B, and Fig. 8e-f shows the wear morphology of specimen-C. The wear track width corresponds to 504 μm , 684 μm , and 1191 μm in specimen-A, specimen-B and specimen-C, respectively.

The wear track of specimen-A was found almost free of wear debris, and corrosion products. However, it contained well defined grooves and sticking of fragmented wear products (Fig. 8a, b). The wear surface of the specimen-B also showed specific plastically deformed wear grooves, and large corrosion products (polygonal particles). These results are indicative that wear mechanism in specimen-A and specimen-B is predominantly abrasive wear type [29].

As illustrated in Fig. 8e-f, the wear track formed on the specimen-C showed heterogeneous distribution of polygonal agglomerates of wear and oxidation products. Other than the wear grooves some large worn patches were also observed, those might have been developed due to the adhesive wear mechanism. A detailed and magnified overview of worn surface and retained wear debris has been shown in Fig. 9. EDX spectrum given in Fig. 9d confirmed the presence of Fe based oxides; those might have been formed due to the atmospheric oxidation of Fe present inside the surface layer.

The depth and width of wear track of each specimen obtained after 2000 m sliding distance has been shown in Fig. 10. It is event that depth and width of the wear track showed almost a linear relationship and an increasing trend from specimen-A to specimen-C. This behavior is in good agreement with the microhardness profile of laser melted zone of the respective specimens. As the depth of the melted zone is increased, the concentration of iron atoms (Fe) gets increased in the coating layer, whereas the fraction of Ni_3Al particles gets decreased. Therefore, the resistance in wear also gets decreased as a result of dilution of hard Ni_3Al coating particles.

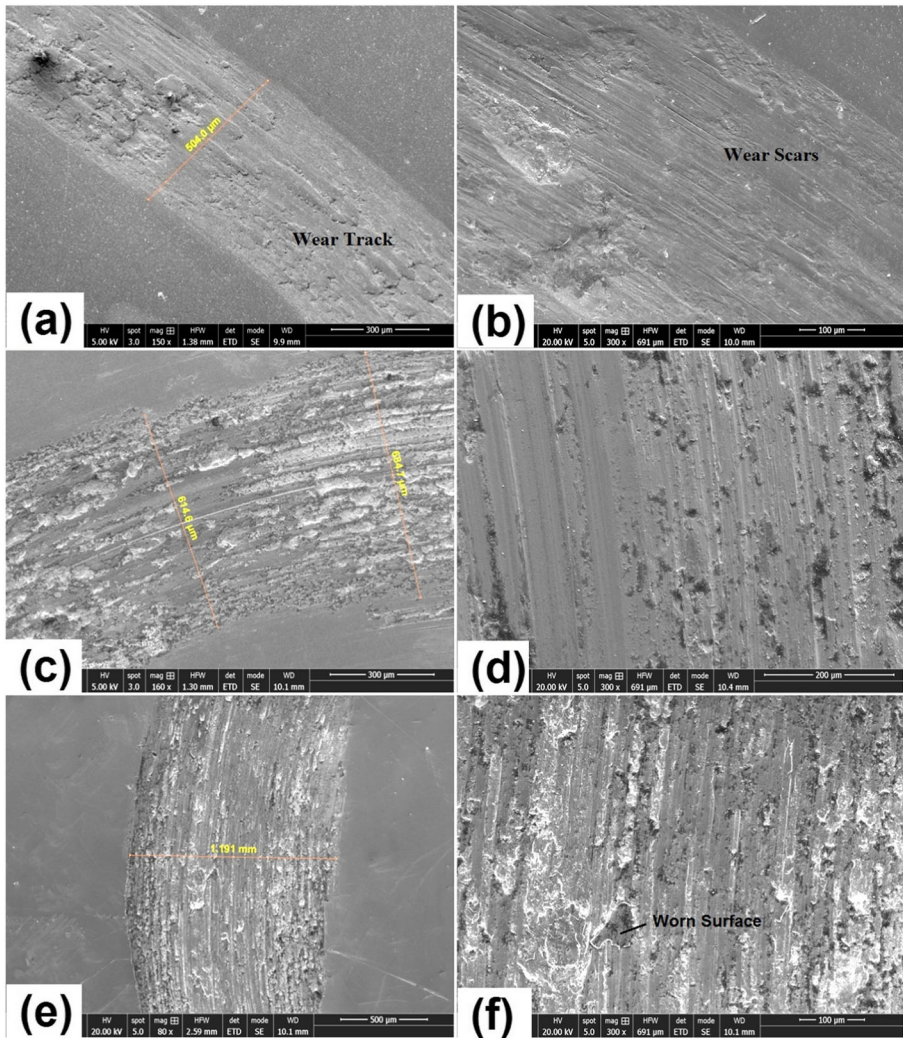


Fig. 8 SEM micrographs of wear track at low and high magnifications, **a–b** specimen-A, **c–d** specimen-B, **e–f** specimen-C

Conclusions

In this study the effect of laser re-melting on the microstructure and wear properties of plasma sprayed Ni_3Al coatings was studied. Following conclusions could be drawn from the experimental results and the above made discussion.

1. The laser re-melting process improved the microstructure of the nickel-aluminide coatings, and reduced the roughness and porosity of the coatings significantly. Similarly, coating-substrate interface was improved and a metallurgical bond was formed as a result of laser re-melting and controlled solidification.

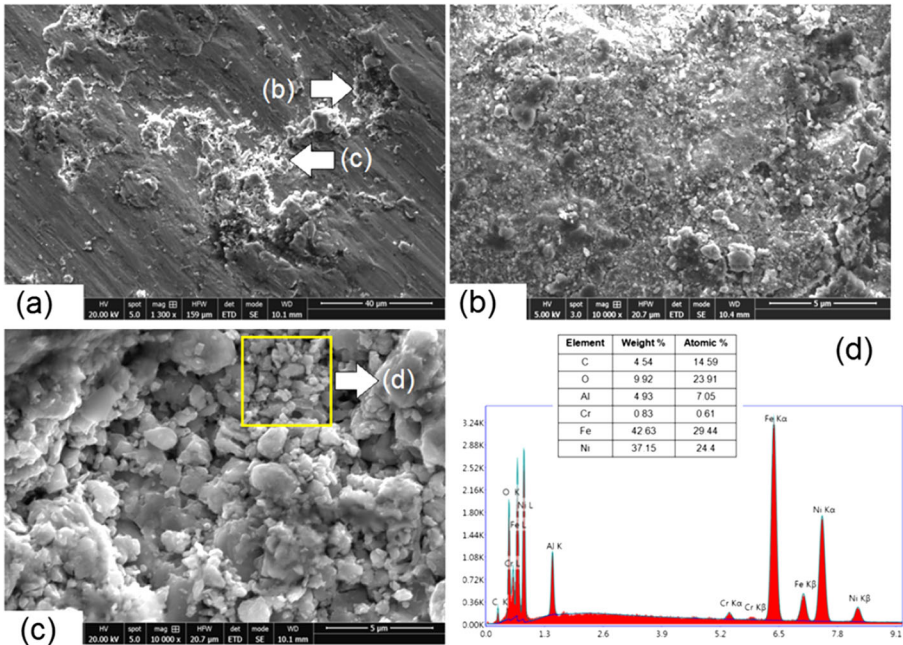


Fig. 9 Detailed SEM and EDX spectrum of wear debris/worn out surface (Specimen-C)

- The dispersion of Ni_3Al particles inside the substrate matrix has a positive effect on the microhardness, and wear properties of the modified surface. The microhardness of the laser treated surface get enhanced $\sim 200\%$ with respect to the bulk of the material.
- The wear rate of the laser treated surface was increased with the decreasing Ni_3Al content of the modified surface (by increasing the depth of laser melted zone). This relationship signifies that the higher concentration fraction of Ni_3Al hard particles improves the wear resistance of the modified composite layer.

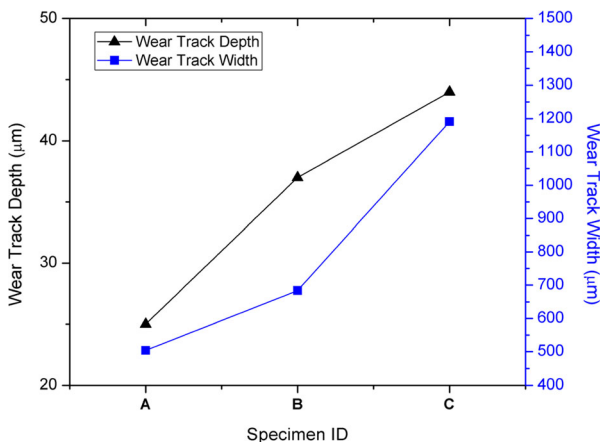


Fig. 10 Depth and width of the wear track in laser treated specimens

4. The wear mechanism in the laser treated specimens was found to be the ploughing and scratching. Moreover, the depth and width of the wear track got increased as the depth of the melted zone increased in the laser treated specimen. The EDX analysis of the wear debris confirmed the existence of Fe containing oxidation products, which is also a confirmation of Fe migration/diffusion into the surface coatings layer as a result of deep penetration of laser beam.

References

1. Culha, O., Celik, E., Azem, N.A., Birlık, I., Toparli, M., Turk, A.: Microstructural, thermal and mechanical properties of HVOF sprayed Ni–Al-based bond coatings on stainless steel substrate. *J Mater Process Technol.* **204**(1-3), 221–230 (2008)
2. Kim, H.J., Hwang, S.Y., Lee, C.H., Juvanon, P.: Assessment of wear performance of flame sprayed and fused Ni-based coatings. *Surf Coat Technol.* **172**(2-3), 262–269 (2003)
3. Kotoban, D.V., Shishkovskii, I.V.: A study of the structure of nickel aluminide after laser treatment. *Metal Science and Heat Treatment.* **57**(9-10), 603–609 (2016)
4. Burakowski, T., Wierzchon, T.: *Surface Engineering of Metals: Principles, Equipment, Technologies.* CRC press (1998)
5. Ulutan, M., Celik, O.N., Gasan, H., Er, U.: Effect of different surface treatment methods on the friction and wear behavior of AISI 4140 steel. *Journal of Materials Science & Technology.* **26**(3), 251–257 (2010)
6. Tsujikawa, M., Yoshida, D., Yamauchi, N., Ueda, N., Sone, T., Tanaka, S.: Surface material design of 316 stainless steel by combination of low temperature carburizing and nitriding. *Surf Coat Technol.* **200**(1-4), 507–511 (2005)
7. Suh, B.S., Lee, W.J.: Surface hardening of AISI 316L stainless steel using plasma carburizing. *Thin Solid Films.* **295**(1-2), 185–192 (1997)
8. Lakhtin, Y.M., Kogan, Y.D.: Nitriding of steel. *Metal Science and Heat Treatment.* **20**, 250–251 (1978)
9. Kulka, M., Pertek, A.: Microstructure and properties of borided 41Cr4 steel after laser surface modification with re-melting. *Appl Surf Sci.* **214**(1-4), 278–288 (2003)
10. Kulka, M., Pertek, A.: Microstructure and properties of borocarbured 15CrNi6 steel after laser surface modification. *Appl Surf Sci.* **236**(1-4), 98–105 (2004)
11. Li, K., Li, D., Liu, D., Pei, G., Sun, L.: Microstructure evolution and mechanical properties of multiple-layer laser cladding coating of 308L stainless steel. *Appl Surf Sci.* **340**, 143–150 (2015)
12. Fu, Y., Batchelor, A.W., Xing, H., Gu, Y.: Wear behaviour of laser-treated plasma-sprayed ZrO₂ coatings. *Wear.* **210**(1-2), 157–164 (1997)
13. Colaco, R., Gordo, E., Ruiz-Navas, E., Otasevic, M., Vilar, R.: A comparative study of the wear behaviour of sintered and laser surface melted AISI M42 high speed steel diluted with iron. *Wear.* **260**(9-10), 949–956 (2006)
14. Conde, A., Colaço, R., Vilar, R., De Damborenea, J.: Corrosion behaviour of steels after laser surface melting. *Mater Des.* **21**(5), 441–445 (2000)
15. Abboud, J.H., Benyounis, K.Y., Olabi, A.G., Hashmi, M.S.J.: Laser surface treatments of iron-based substrates for automotive application. *J Mater Process Technol.* **182**(1-3), 427–431 (2007)
16. Bartkowski, D., Młynarczyk, A., Piasecki, A., Dudziak, B., Gościański, M., Bartkowska, A.: Microstructure, microhardness and corrosion resistance of Stellite-6 coatings reinforced with WC particles using laser cladding. *Opt Laser Technol.* **68**, 191–201 (2015)
17. Bartkowska, A., Pertek, A., Kulka, M., Klimek, L.: Laser surface modification of boronickelized medium carbon steel. *Opt Laser Technol.* **74**, 145–157 (2015)
18. Mateos, J., Cuetos, J.M., Vijande, R., Fernández, E.: Tribological properties of plasma sprayed and laser remelted 75/25 Cr₃C₂/NiCr coatings. *Tribol Int.* **34**(5), 345–351 (2001)
19. Mateos, J., Cuetos, J.M., Fernández, E., Vijande, R.: Tribological behaviour of plasma-sprayed WC coatings with and without laser remelting. *Wear.* **239**(2), 274–281 (2000)
20. da Silva, W.M., Suarez, M.P., Machado, A.R., Costa, H.L.: Effect of laser surface modification on the micro-abrasive wear resistance of coated cemented carbide tools. *Wear.* **302**(1-2), 1230–1240 (2013)

21. Toboła, D., Brostow, W., Czechowski, K., Rusek, P.: Improvement of wear resistance of some cold working tool steels. *Wear*. **382**, 29–39 (2017)
22. Sidhu, B.S., Puri, D., Prakash, S.: Mechanical and metallurgical properties of plasma sprayed and laser remelted Ni–20Cr and Stellite-6 coatings. *J Mater Process Technol*. **159**(3), 347–355 (2005)
23. Selvan, J.S., Subramanian, K., Nath, A.: Effect of laser surface hardening on En18 (AISI 5135) steel. *J Mater Process Technol*. **91**(1-3), 29–36 (1999)
24. Scott, D.A., Brandt, M., Dorian-Brown, B., Valentine, B., De, P.: Laser modification of metal surfaces. *Opt Lasers Eng*. **18**(1), 1–13 (1993)
25. Weitoa, W., Streiff, R., Maocai, W.: Effect of laser surface modification on high-temperature oxidation and corrosion behaviour of alloys and coatings. *Mater Sci Eng A*. **120**, 499–507 (1989)
26. Šturm, R., Žnidaršič, M., Grum, J.: Crack-growth behavior of laser surface-alloyed low-carbon steel. *J Mater Eng Perform*. **22**(9), 2542–2549 (2013)
27. Serres, N., Hlawka, F., Costil, S., Langlade, C., Machi, F.: An investigation of the mechanical properties and wear resistance of NiCrBSi coatings carried out by in situ laser remelting. *Wear*. **270**(9-10), 640–649 (2011)
28. N. Akhtar, M. Afzal, R. Akhter, Effect of laser remelting on surface composite layer of nickel aluminide coated steel substrate, in: 2018 15th International Bhurban Conference on Applied Sciences and Technology (IBCAST), 2018, pp. 45–50
29. Boas, M., Bamberger, M.: Low load abrasive wear behaviour of plasma spray and laser-melted plasma coatings. *Wear*. **126**(2), 197–210 (1988)